75th International Astronautical Congress (IAC), Milan, Italy, 14-18 October 2024.

IAC-24,A3,IP,189,x84077

Enhancing Additive Manufacturing of Lunar Regolith Ceramics through Magnetic Beneficiation

Maxim Isachenkov[a]*, Raffaele Pisani[b], Antonio Mattia Grande[c], Giuseppe Sala[d]

*[a] *PhD student, Politecnico di Milano, Department of Aerospace Science and Technology, Edificio B14, Via La Masa, 34, 20156 Milano – Italy, maxim.isachenkov@polimi.it*
[b] *MSc student, Politecnico di Milano, Department of Aerospace Science and Technology, Edificio B14, Via La Masa, 34, 20156 Milano – Italy, raffaele1.pisani@mail.polimi.it*
[c] *Professor, Politecnico di Milano, Department of Aerospace Science and Technology, Edificio B12, Via La Masa, 34, 20156 Milano – Italy, antoniomattia.grande@polimi.it*
[d] *Professor, Politecnico di Milano, Department of Aerospace Science and Technology, Edificio B12, Via La Masa, 34, 20156 Milano – Italy, giuseppe.sala@polimi.it*
[*] *Corresponding author.*

Abstract: Lunar regolith is a potential primary resource for In-situ Fabrication and Repair during future crewed lunar exploration missions. Leveraging lunar regolith for in-situ additive manufacturing enables the rapid production of on-demand items, spare parts, instruments, and infrastructure components for lunar bases. This approach offers cost reductions in lunar base construction and maintenance while expanding resource utilization. Among the various AM techniques proposed for in-situ fabrication with lunar regolith, stereolithography-based additive manufacturing stands out as a promising method to create precise, high-density, and robust ceramic parts from lunar regolith. However, the heterogeneous mineral composition of LR presents challenges in its processability through stereolithography-based additive manufacturing, resulting in increased printing time and compromised sinterability. This research aims to investigate the influence of the preliminary beneficiation of the lunar regolith on its printability through digital light processing. Our findings demonstrate that the magnetic beneficiation of lunar regolith can dramatically improve its printability using stereolithography-based additive manufacturing by effectively decreasing exposure time for printing 1 layer from 60 to only 5-10 s, which in turn leads to a 10-fold reduction in printing time. Consequently, this enables the efficient and rapid production of high-dense (94%) and mechanically robust ceramic parts using lunar regolith feedstock. Preliminary mechanical testing showed that ceramic parts 3D-printed with magnetically-beneficiated lunar regolith exhibit a median flexural strength of 120 MPa.

Key words: additive manufacturing, 3D-printing, ISFR, ISRU, Moon exploration, lunar regolith

1. Introduction

The exploration and establishment of sustainable human presence on the lunar surface bring the need to develop innovative and efficient manufacturing techniques that capitalize on in-situ lunar resources. The entire lunar surface is covered in natural material called regolith, which becomes an essential resource for In-Situ Fabrication and Repair (ISFR) on manned lunar missions in the future [1], [2]. Using lunar regolith for additive manufacturing (AM) not only makes it easier to produce necessities, replacement parts, and infrastructure components on demand, but it also lowers the financial and logistical expenses of shipping materials from Earth [3], [4], [5]. Stereolithography-based additive manufacturing (SL-AM), and more specifically, the Digital Light Processing (DLP) technique is one of the AM approaches that has been explored recently and has shown promising results for the manufacturing of high-precision, dense, and structurally robust ceramic components directly from lunar regolith [6], [7], [8], [9], [10]. This technique involves the selective curing of a liquid photopolymer resin mixed with lunar regolith particles, followed by a post-curing and sintering process to achieve the dense ceramic material with the desired mechanical properties and microstructure.

Despite its potential, utilization of DLP AM with lunar regolith feedstock brings up several technical challenges, primarily due to the heterogeneous mineral composition of this natural material. Compositional variations of the regolith can significantly affect its processability during the DLP process, leading to unwanted effects such as

insufficient UV-light penetration into the regolith-containing slurry, prolonged printing times, and suboptimal sintering results [6]. As sinterability directly influences the mechanical integrity and microstructure of the final 3D-printed ceramic components, addressing these challenges is crucial for the successful implementation of DLP AM in the lunar environment.

To overcome these challenges, beneficiation of lunar regolith—refining the raw material to improve its homogeneity by refining its mineral composition has been proposed as a critical step prior to its use in various ISRU technologies, including oxygen production [11], glass manufacturing [12] and metals extraction [13]. However, the possibility to beneficiate of lunar regolith prior to its use as a feedstock for stereolithography-based AM has never been explored.

Beneficiation techniques such as magnetic separation [14] and electrostatic beneficiation [15] can be employed to enhance the homogeneity and consistency of the regolith feedstock, potentially improving its printability through stereolithography AM, its sintering behavior, and the mechanical properties of the final 3D-printed ceramic parts.

This study explores the impact of preliminary magnetic beneficiation of lunar regolith on the printing efficiency and sintering behavior of 3D-printed ceramics. By investigating these parameters, this research aims to advance the understanding and optimization of lunar regolith as a feedstock for stereolithography-based additive manufacturing, ultimately contributing to the feasibility and efficiency of in-situ manufacturing on the Moon.

2. Materials and Methods

For the tests, the Lunar Highlands (LHS-1) and Lunar Mare (LMS-1) simulants were purchased from the University of Central Florida's Exolith lab [16], [17]. The LHS-1 simulant accurately mimics the chemical and mineral composition of lunar highlands, composed mainly from anorthite, whereas the LMS-1 simulates basalt-rich lunar mare soils. Both simulants contain mineral particles ranging in size from 10 to 200 μm, which correlates with data on original Apollo samples [18].

Preliminary milling of the powders was performed using a Retsch PM-100 (Retsch, Germany) ball mill. A Binder ED-56 (Binder, Germany) oven was used to evaporate the isopropyl alcohol, which was used as a milling media. The particle size was measured with a laser diffraction apparatus Mastersizer 2000 (Malvern, UK), measurement range 0.02-2000 μm).

The geometry of the sintered ceramic samples was determined using Filetta IP54 digital caliper, and density was determined through the Archimedes method using OHAUS Pioneer balance with the density measurement set.

To study the samples' microstructure, they were pressed into pellets filled with epoxy resin, flat-ground, and polished on an Allied Metprep PH-3 polishing station. Pellets were plasma-sprayed with a 40 nm layer of gold to ensure that samples would not accumulate charge under the electron beam of SEM.

A 3-point bending test of additively manufactured 40x5x3 mm bars was performed using the MTS 858 Mini Bionix II machine.

3. Experimental

Previously, it was found that the mineral composition of lunar regolith strongly impacts the UV-permeability of lunar regolith-based slurries, utilized for SL-AM [19]. Particularly, it was determined that lighter anorthite-rich highland regolith favours SL-based AM more than a darker basalt-rich mare regolith, absorbing less UV light and, in turn, ensuring greater photo-polymerization depth [20]. Adding to this is the fact that the lunar south pole, where all the prospective manned lunar missions will operate, is mostly constituted by the highland soils, it makes greater sense to focus on enhancing the performance of the anorthite-rich soils, rather than trying to fix the performance of the lunar basalts for the SL-AM processes.

In this regard, our concept of preliminary beneficiation was focused on refining the composition of highland lunar regolith, by enriching the anorthite content in it. As the anorthite itself is non-magnetic, whereas basalt has significant iron content, thus effectively attracts to the magnet.

The LHS-1 was subject to magnetic beneficiation. This process involved spreading the starting LHS powder on a flat surface and using a strong permanent magnet to separate the ferromagnetic particles of basalt and ilmenite from the powders. The separation went through multiple stages, to enable the total separation of the ferromagnetic particles from the bulk of LHS powder. Separation continued until there were no visible ferromagnetic particles attracted to the magnet after immersing it into the starting LHS powder. In the process of magnetic separation, two distinct fractions of the lunar highland regolith were produced - non-magnetic (NM) and magnetic (M) (fig.1).

Figure 1. Magnetic LHS-1M powder (left), non-magnetic LHS-1NM powder (right)

After the separation, both fractions were subjected to sieving and milling. The sieving procedure was carried out in continuous mode for 10 min, using the Octagon D200 Digital Sieve Shaker (Endecotts). Stack of two sieves (280 and 140μm) were fitted. Powder left at the bottom of the sieving machine's tank was taken to the milling procedure.

LHS-1M, LMS-1NM, original LHS-1 and LMS-1 and two additional powder mixtures (95 wt.% NM- 5wt% M and 97.5 wt.% NM- 2.5 wt.%) were independently ground with a planetary mill using yttria-stabilized zirconia (YSZ) milling jars and 2 mm YSZ balls in the presence of isopropyl alcohol (IPA). The mIPA: mpowder ratio was 1.5:1, while mballs: mpowder ratio was 5:1. The rotation speed of the mill was set to 250 rpm. Milling was performed for 120 min. After milling, IPA was evaporated from the samples in an oven at 60 °C for 24 h. The dried powders were collected for further testing. Table 1 describes six resulting powder samples.

Table 1. Description and composition of milled regolith simulant powders, used in the experiments.

Sample name	**Description**	**Anorthite content, wt.%**	**Basalt+ Ilmenite content, wt.%**
LHS-120	milled unrefined highland regolith	75	25
LMS-120	milled unrefined mare regolith	25	75
NM-120	milled non-magnetic fraction of LHS-1	99	<1
M-120	milled magnetic fraction of LHS-1	<1	99
NM_2.5-120	milled NM(97.5%)/M(2.5%) mixture	97.5	2.5
NM_5-120	milled NM (95%)/ M(5%) mixture	95	5

To test the photopolymerization response of the beneficiated lunar regolith, lunar simulant-infilled photocurable resins were prepared. The lunar simulant-infilled resins consisted of the above-described milled powders, di-acrylate-based resin, and a suitable phenyl ketone photoinitiator. The powder ratio in the paste was 70 wt.%. Photopolymerization testing was performed using 405 nm UV flashlight and ELEGOO Mars 4 DLP printer, featuring a 405 nm UV projection system. Square 1x1 cm areas were processed with UV curing of the slurries for 2,5,10,15,30,60 and 120 seconds of exposure. The thickness of the polymerized single-layer samples was measured with Interapid GA thickness gauge (Interapid, Switzerland).

After determining optimal slurry composition, vat-polymerization AM was performed using a Mars 4 DLP-based 3D printer (ELEGOO). STL models of the parts were prepared using Autodesk Fusion CAD software, and G-codes were formulated using Voxeldance Tango software. The layer thickness was set to 20 μm to achieve the finest resolution and better layer adhesion. The exposure time for curing one layer was set to 10s, according to the photo-polymerization depth previously achieved for the corresponding regolith-containing slurries. After each layer was UV-cured, the building platform was raised by 10 mm, allowing a new portion of the slurry to flow under the photopolymerized layer. The manufactured green parts were heat-treated in the air at 600 °C for 2h for debinding and sintered at 1250°C, with 4h of holding time and a heating rate of 2°C/min.

4. Results and Discussion

4.1 Photopolymerization depth tests

As it was anticipated, a non-magnetic fraction of lunar regolith, mostly composed of anorthite showed much better photopolymerization performance: due to the less absorption in the UV range, slurries containing less basalt in infilling powder showed higher polymerization depths.

First tests were conducted with a more powerful UV lamp, with an energy output of 40 mW/cm^2 at 405 nm wavelength, which allowed us to test the darker fractions of lunar regolith, including magnetic fraction of LHS and LMS powder. To visualize the results we have plotted the achieved thickness of the single polymerized layers, produced from the slurries, containing different regolith species from the exposure time under UV irradiation. The results are shown in Figure 2.

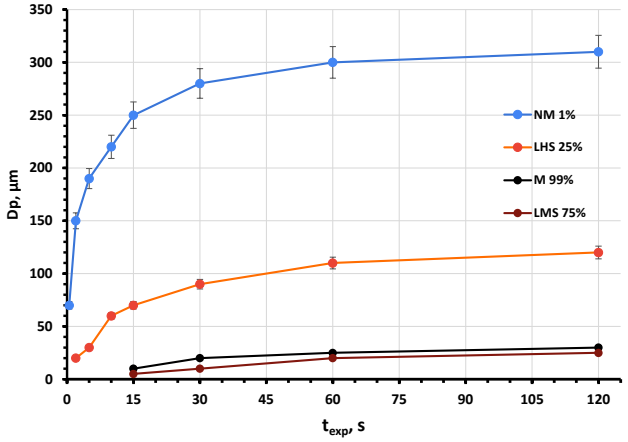

Figure 2. Polymerization depth of regolith-infilled slurries at various exposure times

Figure 2 shows the dramatic difference between the performance of various types of lunar regolith-containing slurries. It was already shown, how mare regolith-containing slurries underperform in DLP printing, compared to highland regolith-based slurries [21], however when compared next to the magnetically beneficiated NM fraction, containing only the trace amounts of basalt, this difference becomes even more significant.

While it takes only 1 second to obtain a 50 µm-thick photopolymerized layer, when using an NM slurry, it will take 15 seconds just to get any signs of polymerization from the slurries, infilled with LMS-120 and M-120 powder, which perform similarly. Original, unrefined LHS-based slurry performs a bit better, however still takes 15x more time (15 s) to reach the same layer thickness (50 µm).

It can be also seen that the maximum photopolymerization depth achievable for the different types of slurries at maximum reasonable exposure time (120 s for a single layer) also differ significantly: while the 315 µm – thick layers can be polymerized from NM-slurry, a normal LHS-based slurry can be hardened only down to 120 µm, while LMS- and M-based compositions can be polymerized no more than for 25 µm, making them almost unusable for DLP-based printing.

Later tests were conducted using the UV projection system of ELEGOO Mars 4 DLP 3D-printer with the measured UV output of 3.7 mW/cm^2 at 405 nm to test the most promising regolith-infilled slurries for the actual DLP-printing on a cheap table-top commercial DLP machine.

The goal here was to study how the subtle differences in basalt content influence the slurry's performance. Herein we have tested NM-slurries with 1-5 wt.% of basalt+ilmenite (M-fraction) content and compared them to the normal LHS-based slurry (with 25 wt.% of basalt+ilmenite), results are plotted in Figure 3.

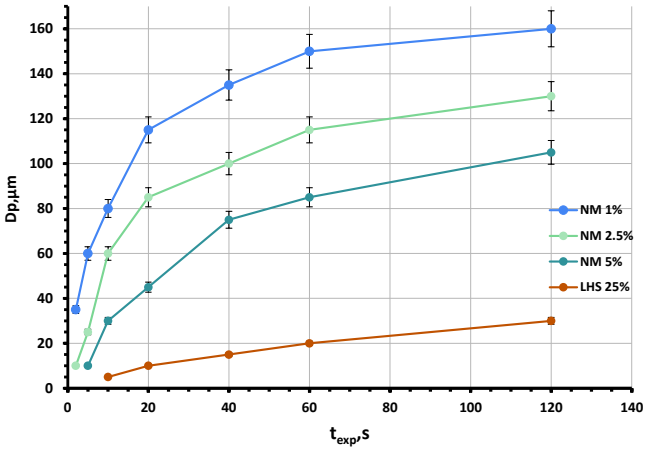

Figure 3. Polymerization depth of regolith-infilled slurries with 1-25% basalt content at various exposure times

Overall the picture is the same as for the more powerful dedicated UV lamp: slurries lower on basalt content show significantly better results for polymerization depths. Also, it can be noticed that even a few presents of basalt significantly lower the polymerization depth. E.g. for 20 s exposure extra 1.5 wt.% of basalt (NM-2.5) lowers D_p by 25% (from 115 down to 85 µm), while the addition of another 2.5 wt.% of basalt (NM-5) lowers it for another 47% (down to 45 µm). To compare, at this exposure time, the original LHS-based slurry with 25 wt.% of basalt can be polymerized only up to 10 µm (which is only 8.7% of the NM-1's result) which is not enough for normal printing operation. For the shorter exposure times, this difference between the different compositions with the varied basalt

content is even higher. Figure 4 shows the basalt content in the slurries influence the printing performance.

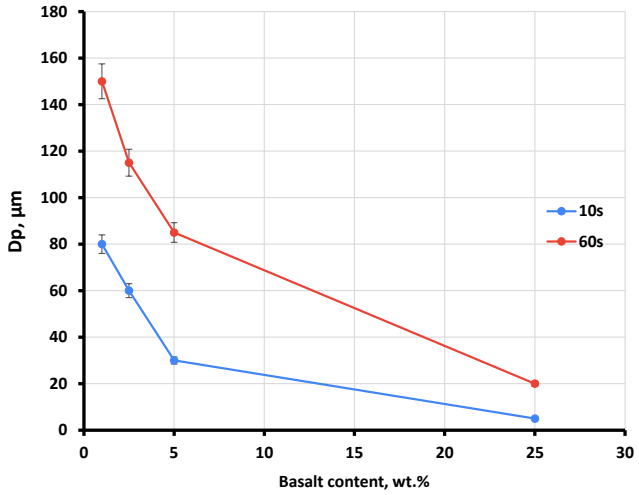

Figure 4. Polymerization depth of regolith-infilled slurries with 1-25% basalt content

It can be seen that both for shorter exposure times (to print faster) and for longer exposures (to print thicker layers) it makes sense to get rid of as much basalt content in the starting regolith powder as possible.

4.2 DLP printing tests

After we have determined the optimal basalt content in the slurry, we have 3D-printed first samples from the NM-120 magnetically beneficiated highland regolith.

Instead of the 60s needed to have a proper inter-layer bonding for the DLP-printing with original highland regolith slurries, it took only 10s to produce properly bonded green parts. With the optimization of the slurry composition, this value can be decreased further.

Produced NM green parts showed a good surface finish, proper interlayer adhesion, and good structural integrity. Obtained green parts and their SEMs are demonstrated in fig.5.

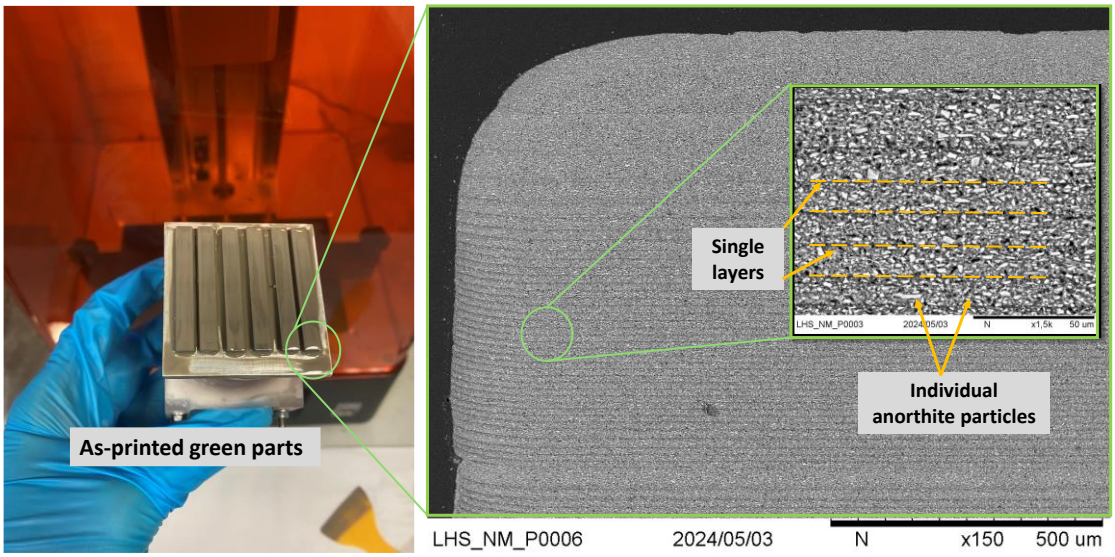

Figure 5. DLP-printed green bodies (left) and their microstructure visible in the SEM (right)

Single 20 µm layers are visible on the SEM with good inter-layer adhesion. Individual anorthite particles, appearing brighter, can be seen inside the polymerized resin matrix (darker background). The structure is crack-free with a smooth surface finish. Only a few visible defects are visible on the produced green part's surface. One can also notice thicker initial layers (on the top side of the part), polymerized with longer exposure times, to ensure good adhesion of the first layers to the building platform.

Printed green parts were subjected to debinding at 600º C with subsequent sintering at 1250º C. We have selected a higher sintering temperature, compared to the one, found in our previous study as an optimal for sintering of highland regolith [6], because the green parts, produced from NM-feedstock contain almost pure anorthite, which has a much higher melting temperature [22], [23], than the anorthite-basalt mixture, found in the original highland regolith. Sintered NM-ceramic parts are shown in the figure 6 next to the green parts:

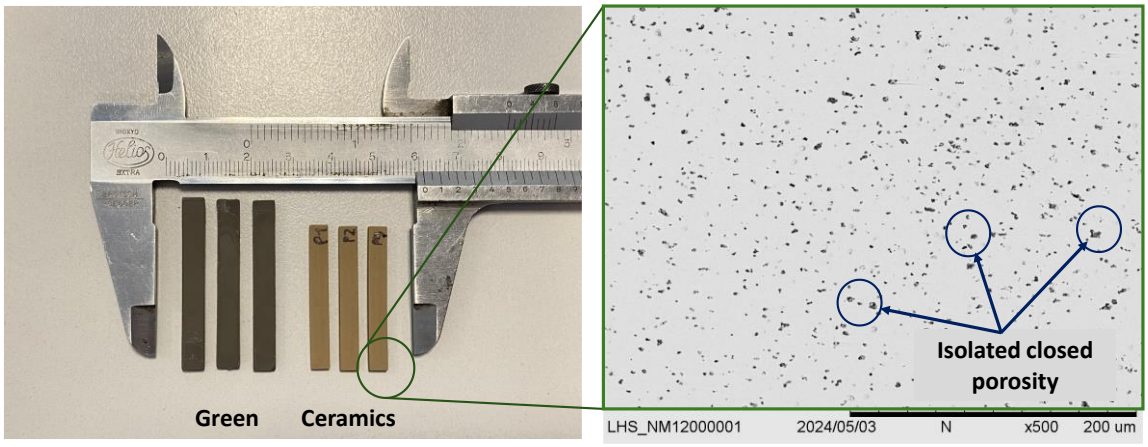

Figure 6. DLP-printed green bodies and sintered ceramic parts (left) and produced ceramic part's microstructure in the SEM (right)

Significant shrinkage of ceramic parts is well visible after sintering, showing effective fusion of individual anorthite grains. It was determined that produced parts have shrunk by **18%** along the X-direction, which shows effective sintering. Produced ceramics reached **94%** of relative density, which is comparable to the results achieved by the other researchers, who exploited stereolithography-based AM with lunar regolith feedstock [24], [25], [26]. SEM micrograph of the polished ceramic bar's cross-section supports this value, as only the individual closed porosity can be observed.

We have made a preliminary characterization of the specimens' ultimate flexural strength by carrying out the three-point bending test. After testing five specimens, we obtained a mean ultimate flexural strength of **120±5 MPa**. Based on a small set of tested specimens, these results suggest that the 3-point bending strength may be in the same range or possibly slightly higher compared to the values obtained by other authors [26], [27].

After we were able to manufacture mechanically-sound ceramic parts with simple geometries, using NM-feedstock, we moved to the production of parts with intricate geometry, including complex lattice structures. Some of the produced ceramic samples are shown in Fig. 7.

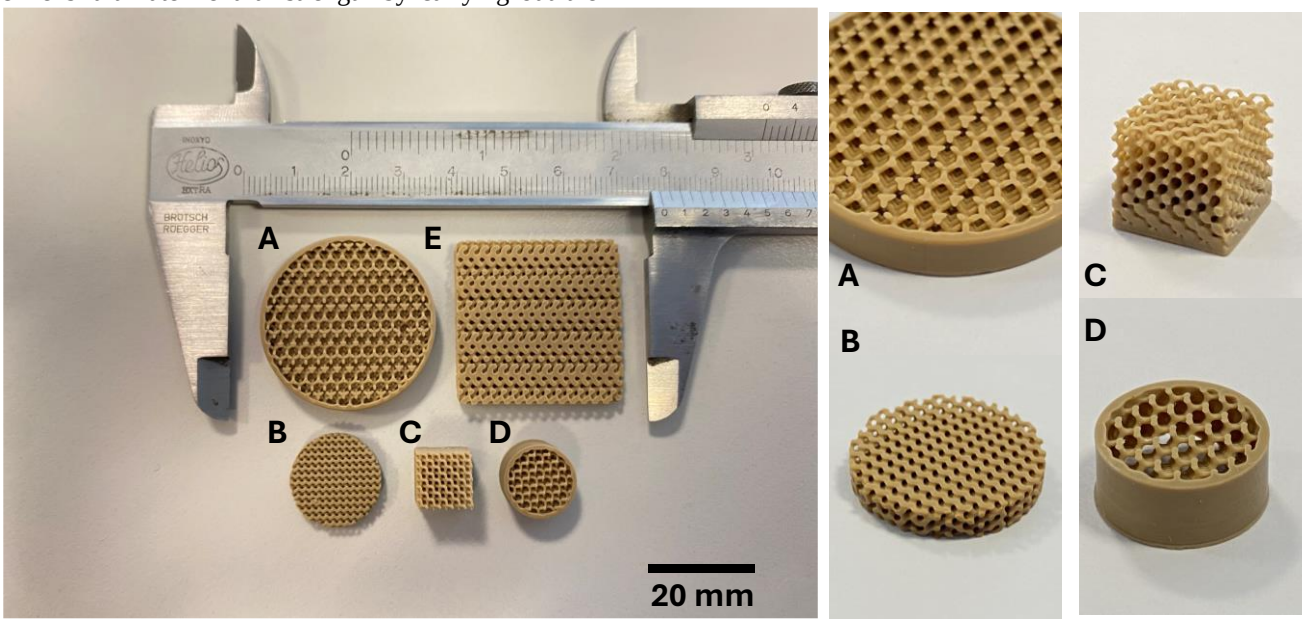

Figure 7. Ceramic lattice structures, DLP-printed from magnetically beneficiated lunar highland regolith simulant.

We were able to successfully produce a number of crack-free ceramic parts with various types of lattices (including gyroids and x-cels). All the printed parts show a smooth surface finish and perfectly preserved the as-designed shape. We tried out both cylindrical and rectangular shapes, with varying lattice infill (10-30 vol.%). Among the produced specimens, sample D has an experimental gradient (5-100%) infill to test the crack behavior of such an intricate geometry.

Based on the good mechanical and thermal properties of anorthite ceramics [28], [29], [30], we can assume that such 3D-printed structures can be utilized in several different fields of lunar exploration and resources prospection. Proposed material can be utilized, where the production of on-demand ceramic parts with low CTE, high temperature, and chemical resistance may be needed, including life support systems (air and water filtration), energy storage (anode material), material recycling (catalysis matrixes) and production of spare parts for scientific instruments and ISRU plants.

5. Conclusion

The present study has confirmed that preliminary magnetic beneficiation of lunar regolith may significantly enhance its printability by means of stereolithography-based AM, in particular via DLP technology. It was experimentally proved using a small commercial DLP printer, originally designed to print only with pristine resins, without any ceramic infill. Even though we have used the machine with very limited capabilities for printing ceramic materials some significant results were successfully achieved. It was found that:

- Regolith magnetic beneficiation helps to obtain a non-magnetic fraction of lunar regolith, mostly consisting of anorthite, that has much lower UV absorption, which in turn leads to a dramatic increase in UV penetration into the slurries used in stereolithography-based AM.

- It helps to drastically reduce the printing time (**up to 10 times**). Depending on the optimal retraction speed, exposure for 1 layer may be decreased from 60 to 5-10 s, compared to original highland regolith-based slurries.

- Parts with thicker 50 μm layers may be effectively produced if needed, while it is only possible to work with 20 μm layers, when using original highland regolith feedstock.

- NM-fraction of lunar regolith consists mostly of anorthite, which has a much higher melting temperature (1550 º C, compared to 1200 º C for original highland regolith)

- Magnetic beneficiation helps to bring highly heterogeneous lunar regolith to the much more predictable, almost homogeneous (99% anorthite) composition, which in turn leads to more predictable and consistent physical properties of final ceramic parts, manufactured from refined feedstock. Eventually, it will help for future standardization and certification of produced lunar regolith parts, as their final composition will be similar, disregarding the differences of lunar regolith feedstock's composition at the particular landing/mining site.

- Using more powerful UV-light sources and DLP/SLA printers designed specifically to work with darker powders may increase the printing speed and green parts' quality even further.

Overall, it was shown that the iron-poor anorthosite fraction proves to be an excellent feedstock for ceramic manufacturing via stereolithography-based additive manufacturing, owing to its lower UV absorption and higher melting temperature.

Future research should aim to introduce the beneficiation techniques to other ISRU technologies, such as oxygen and metal extraction, potentially integrating other complementary processes such as electrostatic or triboelectric separation, to optimize the composition of the regolith feedstock further. Additionally, a more comprehensive assessment of the mechanical properties of the sintered ceramics under lunar environmental conditions—such as extreme temperatures and vacuum—will be necessary to fully validate the suitability of the produced components for long-term use.

In summary, this study contributes significantly to the field of aerospace engineering by advancing the understanding and practical application of magnetically beneficiated lunar regolith in stereolithography-based additive manufacturing.

This research did not receive any specific grant from funding agencies in the public, commercial, or not-for-profit sectors.

6. References

[1] R. Romo and C. Andersen, "ISRU: The Basalt Economy," no. November 2016, 2018.

[2] R. Jaumann and W. Seboldt, "A brief review of chemical and mineralogical resources on the Moon and likely initial in situ resource utilization (ISRU) applications," vol. 74, pp. 42–48, 2012, doi: 10.1016/j.pss.2012.08.012.

[3] M. H. Rahman, A. Hayes, K. Muralidharan, D. A. Loy, and M. Shafae, "Towards Lunar In-Situ Resource Utilization and In-Space Manufacturing: Additive Manufacturing of Hydrogel-Based Lunar Regolith Pastes," *SSRN Electronic Journal*, 2023, doi: 10.2139/ssrn.4354354.

[4] E. Sacco and S. K. Moon, "Additive manufacturing for space: status and promises," *International Journal of Advanced Manufacturing Technology*, 2019, doi: 10.1007/s00170-019-03786-z.

[5] M. Isachenkov, S. Chugunov, I. Akhatov, and I. Shishkovsky, "Regolith-based additive manufacturing for sustainable development of lunar infrastructure – An overview," *Acta Astronaut*, vol. 180, no. September 2020, pp. 650–678, Mar. 2021, doi: 10.1016/j.actaastro.2021.01.005.

[6] M. Isachenkov, A. M. Grande, and G. Sala, "Optimizing lunar regolith for vat polymerization and sintering: pre-processing & mineral composition impact," *Ceram Int*, vol. 50, no. 18, pp. 32265–32277, Sep. 2024, doi: 10.1016/j.ceramint.2024.06.034.

[7] C. Wang *et al.*, "Vat photopolymerization of low-titanium lunar regolith simulant for optimal mechanical performance," *Ceram Int*, vol. 48, no. 20, pp. 29752–29762, Oct. 2022, doi: 10.1016/j.ceramint.2022.06.235.

[8] C. Xiao *et al.*, "Additive manufacturing of high solid content lunar regolith simulant paste based on vat photopolymerization and the effect of water addition on paste retention properties," *Addit Manuf*, vol. 71, Jun. 2023, doi: 10.1016/j.addma.2023.103607.

[9] C. Wang *et al.*, "Vat photopolymerization of low-titanium lunar regolith simulant for optimal mechanical performance," *Ceram Int*, vol. 48, no. 20, pp. 29752–29762, Oct. 2022, doi: 10.1016/j.ceramint.2022.06.235.

[10] M. Isachenkov, "Utilization of Stereolithography-based Additive Manufacturing Approach for Manufacturing of Lunar Regolith Ceramics," in *Proceedings of the 73th International Astronautical Congress (IAC), Paris, France, 18-22 September 2022*, Paris: International Astronautical Federation (IAF). All rights reserved., Sep. 2022. Accessed: Sep. 15, 2023. [Online]. Available: https://iafastro.directory/iac/paper/id/70047/summary/

[11] M. F. Franke, "Development of a Testbed for the Beneficiation of Lunar Regolith Concentrating an Ilmenite-Rich Feedstock for In-Situ Oxygen Production on the Moon," Bremen University, 2022.

[12] J. Schleppi, "Manufacture of glass and mirrors from lunar regolith simulant," *J Mater Sci*, vol. 54, no. 5, pp. 3726–3747, 2019, doi: 10.1007/s10853-018-3101-y.

[13] J. N. Rasera, J. J. Cilliers, J. A. Lamamy, and K. Hadler, "The beneficiation of lunar regolith for space resource utilisation: A review," *Planet Space Sci*, vol. 186, no. April 2019, p. 104879, 2020, doi: 10.1016/j.pss.2020.104879.

[14] R. R. Oder, "Beneficiation of lunar soils : Case studies in magnetics," *Min Metall Explor*, vol. 9(3), pp. 119–130, 1992, doi: 10.1007/bf03402983.

[15] W. N. Agosto, "Electrostatic concentration of lunar soil minerals," 1985.

[16] U. of C. F. Exolith Labs, "LHS-1 Lunar Highland Simulant spec sheet," 2021.

[17] U. of C. F. Exolith Labs, "LMS-1 Lunar Mare Simulant spec sheet," 2021.

[18] M. Isachenkov *et al.*, "Characterization of novel lunar highland and mare simulants for ISRU research applications," *Icarus*, vol. 376, no. December 2021, p. 114873, 2022, doi: 10.1016/j.icarus.2021.114873.

[19] M. Isachenkov, S. Chugunov, A. Smirnov, A. Kholodkova, I. Akhatov, and I. Shishkovsky, "The effect of particle size of highland and mare lunar regolith simulants on their printability in vat

polymerisation additive manufacturing," *Ceram Int*, vol. 48, no. 23, pp. 34713–34719, Dec. 2022, doi: 10.1016/J.CERAMINT.2022.08.060.

[20] M. Isachenkov, O. Dubinin, S. Chugunov, I. Akhatov, and I. Shishkovsky, "Digital light processing of complex shape ceramic parts from lunar regolith simulant," in *Proceedings of the International Astronautical Congress, IAC*, 2021.

[21] M. Isachenkov, S. Chugunov, A. Smirnov, A. Kholodkova, I. Akhatov, and I. Shishkovsky, "The effect of particle size of highland and mare lunar regolith simulants on their printability in vat polymerisation additive manufacturing," *Ceram Int*, vol. 48, no. 23, pp. 34713–34719, Dec. 2022, doi: 10.1016/J.CERAMINT.2022.08.060.

[22] M. R. Boudchicha, S. Achour, and A. Harabi, "Crystallization and sintering of cordierite and anorthite based binary ceramics."

[23] J. R. Goldsmith, "The melting and breakdown reactions of anorthite at high pressures and temperatures," *American Mineralogist*, vol. 65, pp. 272–284, 1980.

[24] H. Chen, G. Nie, Y. Li, X. Zong, and S. Wu, "Improving relative density and mechanical strength of lunar regolith structures via DLP-stereolithography integrated with powder surface modification process," *Ceram Int*, vol. 48, no. 18, pp. 26874–26883, Sep. 2022, doi: 10.1016/j.ceramint.2022.05.390.

[25] B. A. Aguiar, A. Nisar, T. Thomas, C. Zhang, and A. Agarwal, "In-situ resource utilization of lunar highlands regolith via additive manufacturing using digital light processing," *Ceram Int*, vol. 49, no. 11, pp. 17283–17295, Jun. 2023, doi: 10.1016/J.CERAMINT.2023.02.095.

[26] R. Dou *et al.*, "Sintering of lunar regolith structures fabricated via digital light processing," *Ceram Int*, vol. 45, no. 14, pp. 17210–17215, 2019, doi: 10.1016/j.ceramint.2019.05.276.

[27] H. Chen, G. Nie, Y. Li, X. Zong, and S. Wu, "Improving relative density and mechanical strength of lunar regolith structures via DLP-stereolithography integrated with powder surface modification process," *Ceram Int*, vol. 48, no. 18, pp. 26874–26883, Sep. 2022, doi: 10.1016/j.ceramint.2022.05.390.

[28] A. Harabi *et al.*, "Mechanical properties of anorthite based ceramics prepared from kaolin DD2 and calcite," *Ceramica*, vol. 63, no. 367, pp. 311–317, Jul. 2017, doi: 10.1590/0366-69132017633672020.

[29] S. Sittiakkaranon, "Thermal Shock Resistance of Mullite-Cordierite Ceramics from Kaolin, Talc and Alumina Raw Materials," 2019. [Online]. Available: www.sciencedirect.comwww.materialstoday.com/proceedings

[30] J. Kim, S. Hwang, W. Sung, and H. Kim, "Thermal and dielectric properties of glass-ceramics sintered based on diopside and anorthite composition," *J Electroceram*, vol. 23, no. 2–4, pp. 209–213, Oct. 2009, doi: 10.1007/s10832-007-9395-9.